Environ Geol (2006) 49: 1139–1155
DOI 10.1007/s00254-005-0158-0

ORIGINAL ARTICLE

P. Fulignati
A. Sbrana
R. Clocchiatti
W. Luperini

Environmental impact of the acid fumarolic plume of a passively degassing volcano (Vulcano Island, Italy)

Received: 28 July 2005
Accepted: 19 November 2005
Published online: 7 March 2006

P. Fulignati (✉) · A. Sbrana · W. Luperini
Dipartimento di Scienze della Terra,
University of Pisa, Via S. Maria 53,
56126 Pisa, Italy
E-mail: fulignati@dst.unipi.it

R. Clocchiatti
Laboratoire Pierre Sue, Bat. 637,
CEA-CNRS, Saclay,
91191 Gif Sur Yvette, France

Abstract This paper investigates the role played by the fumarolic plume of a passive degassing volcano in the genesis of rock coatings (RC) and in the introduction and re-distribution of metals and trace elements in the surficial environment. At La Fossa active volcano (Vulcano Island) and in the surrounding environment RC develop owing to exposure of the ground surface to the volcanic acid plume produced by the passive degassing of La Fossa. Significant positive anomalies of a wide variety of metals and trace elements (including Bi, Ag, Se, Te, Sb, Pb, As, Cu, Tl and Cd) were observed either in distal and proximal RC. Most of these anomalies are interpreted to be the result of the transport and subsequent deposition of trace elements, likely to form volatile compounds, in the fumarolic plume. Two main processes seem to control the geochemistry of RC: one is represented by the leaching and subsequent deposition of elements from the proximal toward the distal RC; the other is the direct input of trace elements carried by the emitted volcanic aerosol. The fact that most of the trace elements (particularly Pb, As, Tl, Bi, Te, Se, Cd) enriched in the RC of Vulcano are highly toxic and potentially dangerous to health in high concentration, indicates that the atmospheric metal injection by the quiescently degassing La Fossa volcano together with the subsequent deposition and remobilization by means of surficial waters may represent an environmental hazard that should be taken into account in evaluating the potential impact of volcanic air pollution on human health.

Keywords Rock coatings · Fumarolic plume · Acid gases · Trace metals · Vulcano

Introduction

Active volcanoes play a key role in the cycling of volatile elements between the Earth's interior and its surface, and volcanic emissions constitute a significant natural source for many chemicals, such as SO_2, H_2S, HCl, HF, CO_2, H_2O, metals and trace elements. Several works report that metal and trace element transport by means of low-pressure fumarolic fluids in volcanic systems, characterized by passive degassing, is not sufficient to give significant anomalies, and the metal flux from these systems appears inadequate as a potential ore-forming fluid (Hedenquist et al. 1994; Hedenquist 1995). The transport of significant amounts of metals and trace elements by fumarolic fluids is, however, testified by incrustations and sublimates present surrounding high-temperature fumarolic vents (Symonds et al. 1987; Symonds 1992; Kavalieris 1994; Korzhinsky et al. 1994; Fulignati and Sbrana 1998; Taran et al. 1995, 2000), by the sublimates collected in silica tubes placed in fumaroles (Le Guern 1988; Bernard et al. 1990; Garavelli et al. 1997; Cheynet et al. 2000; Zelenski and Bortnik-

ova 2005), and from the bioindicator investigation of lichens (Grasso et al. 1999; Varrica et al. 2000).

In recent decades the transport of metals and trace elements in the fumarolic plumes of active volcanoes, their injection into the atmosphere and their importance in the understanding of the global biogeochemical cycle have been the subject of numerous papers (Buat-Menard and Arnold 1978; Zoller et al. 1983; Gemmel 1987; Symonds et al. 1987, 1990, 1994; Quisefit et al. 1989; Bernard et al. 1990; Le Cloarec et al. 1992; Symonds 1992; Symonds and Reed 1993; Hinkley et al. 1994; Taran et al. 1995, 2000; Gauthier and Le Cloarec 1998; Allard et al. 2000; Delmelle 2003; Pyle and Mather 2003). All these works report that the elements typically carried by fumarolic fluids are Hg, Se, Te, Re, Tl, Bi, Cd, Au, Br, Pb, W, Mo, V, Cs, Sn, Ag, As, Zn, Rb, Cu, Li, Sb, K and Na. At least a substantial proportion of these elements (for example, Te, Se, Bi, Cd, Re, Au, Br, Pb, W, Mo, Cs, Sn, Ag and Hg) are considered to be of magmatic origin (Symonds et al. 1987; Symonds and Reed 1993). Most of the trace elements are volatilized from shallow degassing magma as simple chlorides. Some elements may also reside in other gas species as sulfides, oxyacids, oxyhalides, hydroxides, hydrides and as native elements. The speciation of each volatile element depends on the bulk gas composition. Near-surface cooling of the gases triggers precipitation of the trace elements in the order of their saturation temperature as sublimates. These are typically oxides, halides, sulfides, tungstates and native elements. Symonds (1992) and Symonds and Reed (1993) calculated that equilibrium cooling of the gases to 100°C causes >99% of the trace elements to be removed from the gas by sublimation, with the exception of Hg, Sb and Se. However, significant quantities of metals, metalloids and trace elements are also injected into the atmosphere by

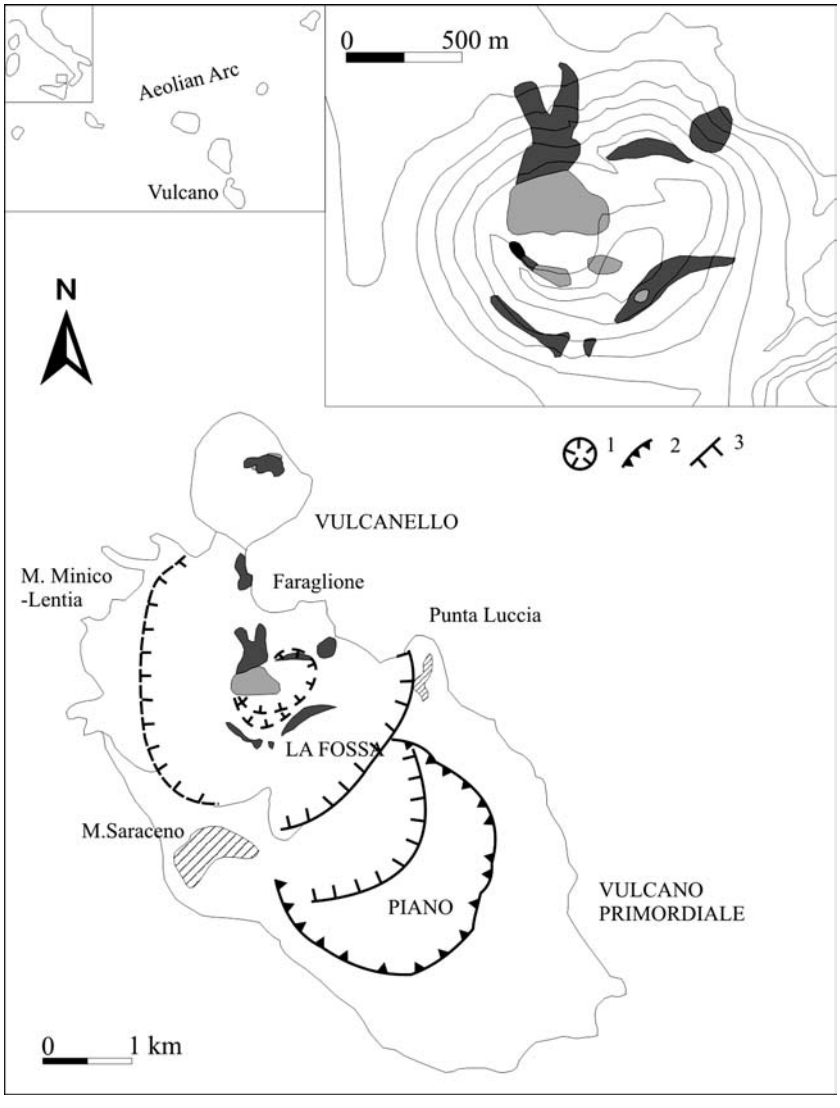

Fig. 1 Sketch map (modified after Keller 1980) of Vulcano Island and the areal distribution of the surficial hydrothermal alteration facies. *Light gray areas* silicic alteration facies; *dark gray areas* advanced argillic (alunitic) alteration; *black area* intermediate argillic alteration; *ruled areas* fossil hydrothermal alteration (advanced argillic type). *1* Crater rims; *2* Piano caldera rim; *3* La Fossa caldera border faults

quiescently degassing volcanoes; an annual amount of about 10,000 tons is estimated (Hinkley et al. 1999; Delmelle 2003). The contribution of these elements to the atmosphere implies several evidences discernible on a global scale. That volcanic emissions influence the levels of these elements in the atmosphere (Nriagu 1989; Hinkley et al. 1999; Pyle and Mather 2003) and their deposition on the earth surface is revealed by the analysis of trace elements in ice cores (Matsumoto and Hinkley 2001) and snow deposited in a wide area of Antarctica (Zreda-Gostynska et al. 1997). The atmospheric load may in turn influence the oceanic concentrations and induce distinctive depth–concentration profiles (Murozumi 1992). Furthermore, the volcanogenic introduction of significant amounts of these trace elements in the surficial environment represents a potentially relevant aspect from the point of view of environmental impact (Laroque et al.1998; Allen et al. 2000; Armienta et al. 1998, 2002; Delmelle 2003).

This paper reports on the areal distribution of metals and trace elements fixed at ground by rock coatings (RC) developed in the region surrounding La Fossa volcano, and considers the evidence that the fumarolic plume of a passively degassing volcano is strongly implicated in the deposition and redistribution of metals and trace elements also at the scale of a single volcanic center. There may be potentially important implications regarding public health hazard on Vulcano Island in consequence of the revelations of this study. If the continuous fumarolic activity of La Fossa volcano throughout the last century is considered, the implication arises that the local population has suffered a long-term exposure to harmful compounds.

The magmatic-hydrothermal system of Vulcano

The active volcanic center of Vulcano Island, which is a part of the Quaternary Aeolian Island Arc, is La Fossa cone (Fig. 1) located inside "La Fossa caldera", a volcano-tectonic pull-apart structure (Ventura 1994). Since the last eruption, which occurred in 1888–1890, La Fossa has behaved as a passively degassing volcano showing fumarolic activity, particularly intense in the 1920s and also from 1978 until the present day (Barberi et al. 1991). A high-temperature fumarolic field, registering temperatures up to 700°C in the early 1990s, is located on the northern side of La Fossa crater. The redox conditions of the high-temperature fumarolic fluids are governed by the SO_2–H_2S gas buffer (Chiodini et al. 1993). Water and the acid gases (SO_2, H_2S, HCl and HF) discharged from the fumarolic vents are dominated by the magmatic component (Bolognesi and D'Amore 1993; Chiodini et al. 1993, 1995; Capasso et al. 1997) which originates from the degassing of the shallow (2,000–3,000 m of depth) magmatic reservoir of La Fossa volcano (Gioncada et al. 1998). The strong fumarolic activity with hypogenic introduction of acid gases is at the base of an identified active high-sulfidation hydrothermal system identified on the island (Fulignati et al. 1998). The surficial hydrothermal alteration facies found at Vulcano reflects strongly acid conditions. Silicic alteration is mainly developed on the northern side of La Fossa crater corresponding to the area of the high-temperature fumarolic field (Figs. 1, 2) and is characterized by the complete leaching of the protholith under pH < 2, which leaves altered rocks characterized by a composition of $SiO_2 > 90$–95 wt% (Fulignati et al. 1998).

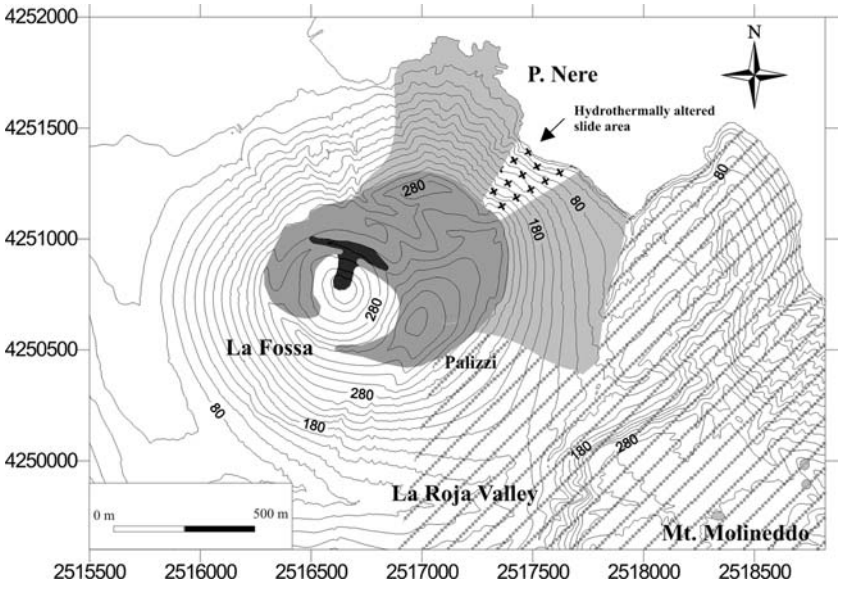

Fig. 2 Areal distribution of the RC in the La Fossa volcano zone. *Black* high-temperature fumarolic field; *dark gray* proximal RC; *light gray* distal RC; *ruled* areas affected by minor RC development (modified after Fulignati et al. 2002)

Advanced argillic (alunitic) alteration is developed laterally to the silicic zone (Fig. 1). The advanced argillic alteration facies mainly consists of alunite and supergene gypsum and jarosite. A very small area of intermediate argillic alteration (halloysite–smectite–goethite paragenesis) occurs inside the western side of the crater as a transition from the advanced argillic alteration (Fig. 1).

In addition to fluids and acid gases, the high-temperature fumaroles of La Fossa introduce metals and trace elements into the surficial environment, as shown by studies on the hydrothermally altered rocks and precipitated sublimates surrounding the vents and lichens used as bioindicators (Garavelli et al. 1997; Sortino and Bichler 1997; Fulignati and Sbrana 1998; Grasso et al. 1999; Varrica et al. 2000; Cheynet et al. 2000). These papers report the occurrence of compounds bearing Pb, Bi, Zn, Cd, Fe, Au, Ag, Cu, Te, Se, Sb, Co, V, Hg, Cr, Tl, As, F, Br, Cl, S and B in the fumarolic fluids, and in particular Cheynet et al. (2000) estimated the following ranges for the elemental rates of transport (g/day): 2.6×10^{2}–4.8×10^{1} Tl; 2.6×10^{2}–4.8×10^{1} Cd; 9.0×10^{2}–1.7×10^{2} Zn; 2.4×10^{3}–4.4×10^{2} Bi; 1.3×10^{4}–2.5×10^{3} Pb; 1.4×10^{4}–2.5×10^{3} As.

Table 1 Chemical composition of proximal rock coatings (RC)

	W11	W12	W13	W14	W15	W16	W17	W20	W24	W25	W26	W27	W28	W29	W30	W31	W31bis	W49
SiO_2	77.35	72.20	79.50	72.66	71.73	75.61	68.20	70.40	ND	75.03	85.35	74.06	81.17	75.18	77.37	87.30	85.03	75.07
Al_2O_3	10.66	11.83	9.88	12.20	12.43	11.82	13.37	13.25	ND	10.68	6.71	11.44	7.92	11.36	9.64	4.21	6.87	9.89
Fe_2O_3	2.36	4.15	1.77	3.67	4.16	2.24	5.32	3.94	ND	4.00	1.50	3.69	2.51	2.92	2.97	1.08	1.05	3.80
MgO	0.56	0.78	0.39	0.96	0.88	0.59	1.41	0.92	ND	0.82	0.28	0.78	0.61	0.77	0.80	0.36	0.28	1.26
CaO	1.42	1.98	1.09	2.07	2.14	1.49	2.77	2.26	ND	1.83	0.82	1.83	1.44	1.86	2.03	0.68	0.75	2.85
Na_2O	2.68	3.10	2.73	3.29	3.07	3.21	3.30	3.43	ND	2.51	1.85	2.77	1.86	2.77	2.35	1.06	1.80	2.41
K_2O	4.13	4.58	3.97	4.36	4.63	4.40	4.45	4.90	ND	4.06	2.83	4.27	3.16	4.31	3.77	1.71	2.96	3.69
TiO_2	0.28	0.35	0.17	0.31	0.34	0.19	0.41	0.32	ND	0.38	0.14	0.36	0.32	0.26	0.28	0.17	0.17	0.33
P_2O_5	0.07	0.21	0.05	0.10	0.16	0.06	0.36	0.17	ND	0.14	0.04	0.13	0.08	0.08	0.11	0.03	0.03	0.13
MnO	0.05	0.08	0.04	0.08	0.08	0.05	0.09	0.08	ND	0.07	0.04	0.07	0.05	0.06	0.06	0.03	0.04	0.08
SO_3	0.45	0.75	0.40	0.31	0.37	0.33	0.30	0.34	ND	0.48	0.46	0.59	0.86	0.43	0.62	3.38	0.56	0.50
Sum	100.01	100.01	99.99	100.01	99.99	99.99	99.98	100.01		100.00	100.02	99.99	99.98	100.00	100.00	100.01	99.54	100.01
LOI	3.96	3.14	4.45	3.64	2.73	3.73	3.05	2.44	ND	4.13	6.20	3.83	6.67	3.96	4.53	19.90	6.01	4.52
F	1234	ND	929	ND	ND	ND	ND	ND	ND	ND	ND	1162	ND	934	ND	1095	ND	966
Li	63.96	54.34	25.53	58.63	59.73	39.18	23.99	23.59	61.46	44.71	21.33	47.86	16.00	51.99	43.98	21.12	45.54	41.82
Be	4.24	6.36	2.43	6.28	6.23	4.80	2.38	2.70	6.64	5.24	1.92	5.63	1.57	6.05	3.24	1.43	2.98	3.28
B	37.88	64.49	16.12	32.59	5.30	19.98	19.99	31.06	73.37	14.36	6.81	38.89	38.51	100.42	20.24	0.78	12.38	32.03
Sc	3.19	7.19	1.26	6.28	6.54	3.27	5.38	3.34	6.18	6.78	0.86	5.47	2.75	5.29	4.78	1.20	1.14	7.31
V	24.58	64.89	8.59	52.26	68.66	20.42	46.10	31.86	57.71	58.37	9.19	51.83	19.34	33.33	32.03	7.54	12.90	51.32
Cr	12.84	26.34	5.39	27.50	27.36	13.27	20.03	14.49	19.77	24.29	6.81	18.04	13.81	13.79	13.61	4.55	4.54	21.23
Co	3.22	8.60	1.37	8.29	9.79	3.97	3.50	3.78	7.52	7.31	1.06	6.71	2.71	5.48	5.25	0.82	1.28	7.96
Ni	5.75	7.67	2.37	11.41	9.59	6.69	6.63	5.49	6.72	8.92	3.61	5.88	6.72	5.89	4.95	1.54	1.98	7.03
Cu	22	23	18	26	28	18	33	25	22	33	17	33	29	29	29	17	18	36
Zn	34.64	79.75	20.21	126.66	98.87	70.40	43.56	39.44	71.55	83.37	18.59	65.68	30.59	50.79	37.82	22.54	23.07	45.27
As	31.33	49.24	18.87	71.10	35.86	22.24	23.34	24.49	52.94	120.45	17.98	63.10	17.87	37.99	19.80	209.70	22.57	24.08
Se	0.16	1.57	bdl	1.81	1.46	1.03	0.43	0.10	1.58	1.86	bdl	2.12	0.79	1.05	bdl	28.70	0.33	bdl
Rb	113.58	188.34	103.34	176.64	115.57	156.28	80.84	74.47	143.69	144.29	81.82	149.38	66.11	135.26	109.43	55.06	92.01	111.91
Zr	100.48	223.34	96.07	204.78	203.24	189.14	113.40	115.45	217.28	181.88	71.28	196.73	86.22	193.70	81.27	36.62	68.43	80.55
Mo	2.43	6.39	2.27	6.46	6.11	4.78	3.57	3.55	6.14	5.36	2.09	4.97	2.95	5.08	1.85	0.98	1.56	1.88
Ag	1.72	3.05	0.59	2.84	2.81	2.25	1.02	1.06	2.75	2.36	0.46	2.46	0.79	2.63	1.49	0.67	1.18	1.51
Cd	0.20	0.11	0.15	0.11	0.10	0.07	0.20	0.25	0.09	0.13	0.10	0.15	0.20	0.06	0.15	0.25	0.10	0.15
Sn	2.03	4.52	1.84	4.52	0.27	3.74	2.40	2.21	4.67	4.70	1.47	6.38	2.20	3.78	1.53	1.06	1.54	1.83
Sb	1.21	2.72	1.43	4.86	2.12	1.44	0.58	1.60	1.99	7.02	1.42	7.07	2.67	2.21	0.53	3.14	1.38	0.58
Te	bdl	0.33	bdl	0.64	0.32	0.29	0.12	0.16	0.17	0.38	bdl	0.52	0.09	0.21	bdl	4.39	bdl	bdl
Cs	5.92	10.17	5.01	10.39	4.94	9.48	5.41	4.64	9.80	9.31	4.07	9.56	3.25	9.31	4.66	2.34	4.56	4.05
W	1.56	3.57	1.65	3.33	3.53	3.14	2.96	2.05	3.71	3.05	1.29	3.18	1.64	3.02	1.32	0.76	1.24	1.25
Pb	36	41	41	48	44	40	41	39		51	38	47	46	47	41	17	35	49
Bi	0.37	0.39	0.32	0.99	0.38	0.2	0.15	0.14	0.34	1.76	0.31	0.53	0.23	0.26	0.3	0.69	0.29	0.38
Th	10.93	37.46	16.57	35.02	25.99	33.39	18.83	15.05	37.52	28.93	12.73	33.61	12.36	30.33	9.96	4.74	8.44	9.08
U	4.49	11.68	5.55	11.57	9.22	11.04	4.66	4.85	11.45	9.12	4.19	10.31	4.01	9.24	3.65		3.37	3.42
La	49	60	48	58	63	56	69	69	ND	56	40	56	45	56	49	27	40	53
Ce	82	102	81	93	98	90	114	101	ND	87	64	93	70	88	79	40	64	83
Tl	ND	ND	0.76	ND	ND	ND	ND	ND	ND	ND	ND	ND	ND	ND	ND	0.69	ND	ND

The high LOI values are influenced by the abundance of S and F in the altered rocks, as reported in Fulignati et al. (1998). Total Fe as Fe_2O_3
ND not determined; *bdl* below detection limits

The development of rock coatings at Vulcano

On Vulcano Island rock coatings (RC) form a relatively continuous, thin millimetre- to centimetre-thick cover which cements together the pyroclastics, dense lapilli and bombs of the latest (1888–1890) eruption and, in the surroundings of La Fossa, RC also lies over older volcanics. RC preferentially develop downwind (eastward) of the high-temperature fumarolic field of La Fossa (Fig. 2) in accordance with the spatial distribution of the fumarolic plume. Two different types of RC were identified on the island in proximal and distal zones with respect to the high-temperature fumarolic field (Fulignati et al. 2002). These differ from each other in mineralogy, texture and chemical composition.

Proximal RC affect the coarse-grained pyroclastic deposits of the 1888–1890 eruption. They are mainly composed of silica and have a massive texture reflecting strong leaching processes at the expense of volcaniclastic material.

Distal RC are characterized by jarosite and silica, with a laminated texture, and reflect an interplay of sedimentary, leaching and deposition processes which are less developed with respect to the proximal RC. Distal RC are mainly developed inside drainage rills.

The origin of RC is thought to be related to water/rock interaction processes under low-pH conditions. The

	W50	W51	W52	W55	W56	W58	W59	W60	W62	W63	W64	W66	W67	W68	W69	W70	W71	W72
SiO_2	83.79	73.01	72.69	69.24	70.60	72.61	ND	70.29	63.46	64.73	ND	66.79	67.47	75.05	85.54	77.80	80.86	80.26
Al_2O_3	7.07	10.59	9.97	12.40	11.39	10.02	ND	12.24	12.08	13.61	ND	12.81	13.52	11.21	5.77	9.80	8.88	9.16
Fe_2O_3	1.82	4.65	6.21	6.07	5.35	5.44	ND	4.82	8.45	6.15	ND	6.03	5.16	3.10	1.59	2.51	1.81	2.05
MgO	0.44	1.12	1.49	1.15	1.56	1.65	ND	1.24	0.85	1.76	ND	1.26	1.23	0.75	0.36	0.70	0.36	0.39
CaO	1.09	2.79	3.05	2.69	3.41	3.36	ND	2.72	2.30	3.98	ND	2.75	2.76	1.88	0.87	1.74	0.99	1.09
Na_2O	1.94	2.56	2.01	2.81	2.49	2.19	ND	2.95	3.02	3.18	ND	3.16	3.36	2.79	1.44	2.57	2.47	2.38
K_2O	2.94	3.93	3.27	4.59	3.88	3.37	ND	4.36	5.38	4.78	ND	4.80	4.82	4.26	2.52	3.83	3.73	3.74
TiO_2	0.18	0.34	0.34	0.44	0.41	0.41	ND	0.38	0.51	0.46	ND	0.60	0.39	0.30	0.18	0.27	0.19	0.30
P_2O_5	0.06	0.19	0.27	0.36	0.26	0.25	ND	0.20	0.58	0.42	ND	0.34	0.30	0.11	0.04	0.08	0.04	0.05
MnO	0.04	0.08	0.10	0.08	0.09	0.10	ND	0.08	0.08	0.10	ND	0.11	0.10	0.07	0.04	0.06	0.04	0.05
SO_3	0.62	0.73	0.61	0.17	0.56	0.61	ND	0.71	3.28	0.83	ND	1.35	0.89	0.48	1.66	0.65	0.64	0.54
Sum	99.99	99.99	100.01	100.00	100.00	100.01		99.99	99.99	100.00		100.00	100.00	100.00	100.01	100.01	100.01	100.01
LOI	6.28	4.29	5.22	4.34	3.85	5.15	ND	3.78	5.19	3.04	ND	4.15	32.67	3.75	10.12	4.48	4.68	3.99
F	871	ND	ND	1035	ND	ND	ND	ND	923	ND	ND	ND	ND	ND	ND	ND	ND	ND
Li	15.16	39.91	37.06	42.88	16.13	36.65	7.36	51.62	22.72	17.30	11.52	57.95	39.91	52.30	22.26	52.17	74.88	86.76
Be	1.44	4.65	3.11	5.09	1.67	2.92	0.69	5.70	2.14	1.95	3.53	6.39	5.31	5.91	3.02	5.66	4.72	5.72
B	17.29	9.98	7.61	8.81	23.63	34.79	13.73	26.19	12.54	23.53	19.18	48.76	43.47	35.38	9.23	12.07	92.88	82.94
Sc	1.69	8.17	6.90	8.51	6.00	7.98	4.43	9.54	4.53	7.36	6.09	9.04	6.92	6.32	2.53	6.12	1.90	2.63
V	12.23	65.22	65.57	87.44	50.73	74.58	30.95	83.55	47.67	58.85	45.99	79.92	59.07	38.70	16.94	30.83	19.77	26.38
Cr	8.54	22.90	23.75	29.96	17.93	28.05	23.81	27.78	14.94	29.65	17.75	32.49	24.91	20.61	7.12	17.15	7.32	8.46
Co	1.66	9.75	9.46	10.91	3.44	9.91	0.89	11.29	1.22	3.42	1.28	10.18	8.83	6.55	2.57	6.25	2.10	2.77
Ni	4.57	8.36	8.20	82.26	5.32	9.40	2.99	9.36	3.99	10.45	4.26	10.85	7.97	8.52	2.81	5.72	3.27	3.77
Cu	19	34	43	45	41	46	5	39	35	55	15	29	27	25	12	21	17	19
Zn	20.96	66.71	12.28	79.71	35.64	62.71	22.44	84.70	37.72	50.54	67.46	104.92	73.24	77.41	66.41	58.34	34.73	30.25
As	11.11	34.94	33.82	25.54	16.94	45.67	1.53	25.05	14.05	12.08	8.17	35.06	22.27	16.07	5.44	22.83	13.20	16.09
Se	bdl	1.19	0.44	1.21	0.25	0.58	bdl	1.49	0.11	0.35	0.99	2.00	1.11	1.30	0.94	0.90	0.01	0.26
Rb	61.34	142.20	96.55	116.65	56.90	97.87	41.24	197.16	82.85	67.84	95.70	194.09	139.67	137.38	120.20	150.72	120.13	
Zr	75.43	159.80	65.37	193.04	87.41	70.42	129.71	184.45	100.20	98.42	335.55	214.88	215.15	193.60	129.89	189.75	81.57	85.06
Mo	2.60	5.42	2.52	5.93	2.80	2.59	3.39	5.16	3.69	3.08	9.06	7.84	6.02	5.36	3.35	5.03	1.96	2.41
Ag	0.63	2.12	1.23	2.60	0.72	1.28	1.22	2.78	1.00	1.00	3.84	3.21	2.52	2.50	1.58	2.56	2.02	2.65
Cd	0.20	0.07	0.10	0.18	0.20	0.20	0.25	0.10	0.20	0.20	0.15	0.18	0.10	0.11	0.02	0.09	0.10	0.15
Sn	1.60	3.29	1.62	3.92	1.84	1.61	2.53	3.68	2.18	1.76	7.25	5.24	4.33	4.06	3.02	3.90	1.88	2.13
Sb	0.63	1.77	0.60	1.04	0.69	0.96	0.37	0.91	0.39	0.33	1.31	2.58	2.03	0.98	0.71	1.40	0.45	0.39
Te	bdl	0.31	bdl	0.24	0.09	bdl	0.02	0.28	bdl	0.17	0.30	0.44	0.16	0.13	0.06	0.15	0.03	0.11
Cs	2.59	8.09	5.43	3.36	3.65	4.93	1.00	10.41	4.91	3.33	5.88	9.58	6.29	8.53	6.62	9.16	5.91	6.45
W	1.41	2.40	1.12	3.15	1.52	1.13	1.89	2.89	1.90	1.70	4.79	4.08	3.47	3.24	2.35	3.02	1.43	1.61
Pb	39	51	50	43	59		45	40	52	36	45		35	36	31	37	36	38
Bi	0.11	0.38	0.43	0.35	0.3	0.52	0.095	0.38	0.18	0.11	0.21	0.38	0.15	0.21	0.09	0.13	0.28	0.28
Th	11.42	28.97	8.65	32.66	13.46	9.68	18.63	34.51	19.78	14.72	42.76	39.5	38.8	29.32	23.65	29.05	9.58	9.72
U	3.86	8.81	3.62	9.9	3.41	3.51	3.55	10.37	4.61	3.74	13.88	11.81	12.24	10.31	7.87	9.23	3.77	3.97
La	38	54	57	88	61	56	ND	64	105	71	ND	74	85	55	37	49	48	48
Ce	63	98	100	145	102	98	ND	101	170	119	ND	124	135	97	54	83	76	84
Tl	ND	ND	ND	1.24	ND	ND	ND	ND	ND	ND	ND	ND	ND	0.52	ND	ND	ND	ND

Table 2 Chemical composition of distal RC

	W21	W22	W23	W33	W34	W35	W73	W74	W75	W76	W84
SiO_2	66.40	70.18	51.60	67.08	56.58	62.65	59.62	62.91	61.74	64.30	64.33
Al_2O_3	12.08	13.36	9.88	13.97	14.29	12.45	10.09	9.53	9.86	9.94	10.31
Fe_2O_3	7.23	4.04	17.95	5.65	10.89	8.89	13.41	12	11.96	10.56	10.32
MgO	1.45	1.07	0.96	1.49	1.68	1.37	0.92	0.86	1.49	1.09	1.59
CaO	3.45	1.82	1.99	3.31	3.94	2.85	1.86	2.03	3.18	2.49	3.21
Na_2O	2.51	3.27	1.62	2.61	2.75	2.25	1.87	1.99	1.98	1.85	2.17
K_2O	4.44	4.85	6.64	4.59	5.38	4.99	5.71	4.99	4.63	4.67	3.82
TiO_2	0.45	0.28	0.55	0.45	0.66	0.55	0.60	0.55	0.57	0.54	0.54
P_2O_5	0.64	0.21	1.38	0.32	1.18	0.86	1.36	1.22	0.99	0.94	1.00
MnO	0.09	0.06	0.05	0.09	0.10	0.07	0.08	0.06	0.09	0.07	0.08
SO_3	1.25	0.86	7.38	0.43	2.56	3.06	4.47	3.87	3.52	3.55	2.63
Sum	99.99	100.00	100.00	99.99	100.01	99.99	99.99	100.01	100.01	100.00	100.00
LOI	5.02	2.98	12.02	4.82	6.83	6.99	8.16	7.90	8.32	7.01	21.05
F	ND	ND	3326	ND	3238	2253	ND	ND	ND	ND	ND
Li	16.61	24.63	8.94	22.06	15.57	13.98	18.49	13.26	13.95	10.01	18.09
Be	1.65	2.63	1.03	2.50	2.59	2.15	1.68	1.58	1.48	1.12	3.24
B	26.88	22.71	34.61	15.10	25.31	11.96	20.54	18.08	12.49	3.54	14.80
Sc	5.57	3.22	7.09	4.68	7.11	6.83	3.86	3.76	5.49	5.12	9.48
V	62.60	28.74	75.05	57.20	89.00	64.10	79.56	66.94	77.16	55.50	124.43
Cr	25.01	10.60	29.20	75.12	31.30	23.60	10.97	21.13	18.17	13.70	28.77
Co	7.15	3.15	0.13	9.42	3.42	4.28	1.44	1.89	2.81	0.86	11.63
Ni	6.67	3.59	10.79	51.87	11.73	7.58	3.55	9.33	5.59	4.26	8.96
Cu	65	51	133	105	209	143	110	163	157	136	204
Zn	36.46	29.92	35.86	52.52	50.05	44.21	40.82	39.03	39.62	36.52	83.03
As	17.54	13.75	33.18	9.25	42.73	33.73	75.99	63.33	60.40	45.76	73.79
Se	bdl	0.05	1.06	0.05	2.05	1.43	0.79	1.16	1.12	1.54	5.13
Rb	79.15	127.22	72.31	81.33	80.48	85.18	86.36	75.73	69.86	62.66	104.41
Zr	79.44	74.47	64.71	98.06	103.24	84.75	115.15	87.92	88.13	85.23	136.36
Mo	2.37	3.05	6.15	11.41	6.46	5.75	6.13	7.98	6.22	5.63	8.62
Ag	0.50	0.52	0.57	0.76	0.82	0.61	0.92	0.72	0.67	0.81	2.30
Cd	0.15	0.15	0.25	0.20	0.20	0.20	0.20	0.20	0.20	0.20	0.10
Sn	1.46	2.42	3.23	1.73	3.29	2.10	4.06	4.07	4.55	5.28	3.63
Sb	0.34	0.32	0.32	0.22	0.51	0.37	0.77	0.59	0.55	0.52	0.90
Te	bdl	bdl	0.20	bdl	0.04	bdl	0.02	bdl	0.24	0.28	0.81
Cs	4.62	5.44	3.67	4.18	4.04	5.60	4.50	3.67	4.21	3.85	7.23
W	1.22	1.62	1.61	1.55	1.87	1.78	1.98	1.72	1.77	1.94	2.39
Pb	47	41	99	36	272	226	271	349	396	377	238
Bi	0.78	0.33	5.35	0.41	1.93	1.21	5.62	3.21	12.40	3.22	5.59
Th	12.99	16.33	18.00	12.40	20.38	21.00	23.84	21.94	19.63	19.53	34.90
U	4.51	4.98	3.85	4.91	5.72	5.92	4.52	4.47	4.38	4.12	10.36
La	101	117	245	80	125	152	171	154	148	128	198
Ce	157	191	335	127	165	224	229	220	195	188	303
Tl	ND	ND	23.0	ND	ND	ND	ND	ND	39.0	ND	2.58

The high LOI values are influenced by the abundance of S and F in the altered rocks, as reported in Fulignati et al. (1998). Total Fe as Fe_2O_3

ND not determined; *bdl* below detection limits

fluids involved in the genesis of RC are mainly dew and rain acidified by interaction with the acid volcanic gasses (SO_2, HCl and HF) carried in the fumarolic plume. This observation is supported by noting the areal distribution of RC that corresponds to the orientation of the volcanic plume (Fulignati et al. 2002).

Analytical techniques

Major elements and La and Ce were analyzed by X-ray fluorescence (XRF) using a Philips PW 1480 spectrometer. Fluorine was determined using a fluorine-selective electrode (Dipartimento di Scienze della Terra, University of Pisa). The other trace elements were analyzed by inductively coupled plasma mass-spectrometry (ICP-MS) with a Thermoelectron X7 ICP-MS quadrupole at Pierre Sue Laboratory (Gif Sur Yvette, France). Rare earth elements (REE) and Tl were analyzed on selected samples by ICP-MS with a VG$^{@}$ Elemental Plasma Quad 2 Plus at Dipartimento di Scienze della Terra, University of Pisa.

SEM-EDS investigation were performed using a Philips XL30 apparatus equipped with an EDAX-DX4 energy-dispersive microanalytical system (Dipartimento di Scienze della Terra, University of Pisa) with operating

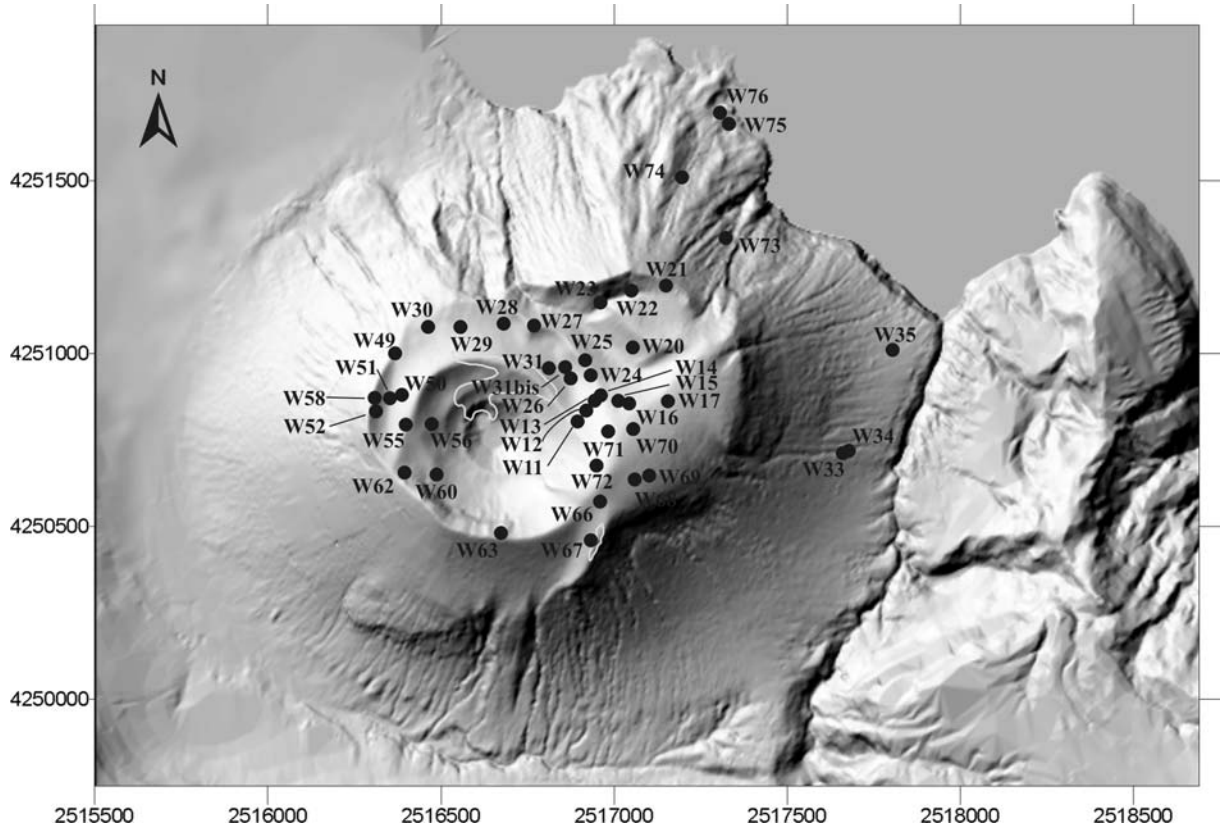

Fig. 3 Location of the samples analyzed in this study

conditions which included a 20 kV voltage and about 0.1 nA beam current.

Results

Analyses of major and trace elements were performed on both the proximal and distal RC. The results are reported in Tables 1 and 2 and the location of the samples is shown in Fig. 3. The major elements are displayed as iso-concentration curves and the trace elements as classed post maps in Figs. 4, 5 and 6. Chemical data show that the proximal RC are characterized by high SiO_2 values > 75–80 wt% (Fig. 4). Conversely all other major elements (Fig. 4; Table 1) are depleted (the high K_2O and Fe_2O_3 values in the small area north of the crater are due to the abundance of alunite group minerals in these samples, Fig. 4). The depletion of major elements becomes less apparent in moving away from the fumarolic field, and distal RC are generally enriched in all major elements (Fig. 4).

High concentrations of a wide set of metals and trace elements are observed both in proximal and distal RC (Figs. 5, 6; Tables 1, 2). Furthermore, sulfur- and chloride-bearing phases containing Cu, Zn, Ag, Pb, Sn, Bi, Fe and Ca and some native elements (Au, Ag and W) were found in proximal RC, whereas chloride-bearing phases containing Pb, Sb, Fe, Ni, Cu, Na, Ca, K and some native elements (Au, Ag and Hg and traces of As and Se as thin concretions on the surface of RC) were found on distal RC (Fig. 7; Table 3). In order to evaluate to what extent elements are enriched in RC, the Enrichment Factor (EF) of Ag, Cd, Sb, Pb, Bi, As, Te, Se, Tl, Sn, La, Ce, Mo, V, Zn, Cu and Ni was calculated for each sample according to the formula (Zoller et al. 1983; Symonds et al. 1987):

$$EF_{sample} = (X/R)_{sample}/(X/R)_{reference}$$

where X and R are respectively the concentration of a given element X and a nonvolatile rock reference element R chosen for normalization in RC and substrate. The choice of the normalization element was problematic because the low-pH environment characteristic of RC formation (particularly proximal RC), implies that most of the elements commonly used for normalization (Mg, Ti and Al; Zoller et al. 1983; Symonds et al. 1987; Taran et al. 1995; Armienta et al. 2002) are leached away. Taking into account the relative immobility of scandium in the silicic alteration facies as observed by Fulignati et al. (1998), this element appeares to be the reference element least affected by leaching processes and is used here for normalization. For the rock source the mean values of the Vulcano rocks on which RC

forms were used. These rocks comprise lapilli, coarse ash and bombs of the 1888–1890 eruption and ashes of the "Pietre Cotte" and "Commenda" eruptions (Clocchiatti et al. 1994; Del Moro et al. 1998; P. Fulignati, unpublished data), and literature data for Ag, Cd, Sn, Te and Se (Govindaraju 1994). The reference data are shown in Table 4. Variable EF values were obtained for proximal and distal RC (Table 5). These values show that several trace elements (Bi, Ag, Se, Te, Sb, Pb, As, Cu, Tl and Cd), typically present in the fumarolic plumes of active degassing volcanoes forming volatile compounds, are particularly enriched in several samples of both proximal and distal RC, reaching EF values up to 10^2–10^3 (Bi, Te, Se, Tl; Fig. 8; Table 5). Some elements, particularly Te, Se, Ag and Sb, reach the highest average and absolute EF values in the proximal RC (Figs. 8, 9; Table 5), whereas Tl, Pb, Bi, As, Cd, Sn and Cu reach the highest EF values in the distal RC (Table 5). Distal RC furthermore show moderate enrichments in La, Ce, V, Mo and Zn (Figs. 8, 9; Table 5) whereas these are generally impoverished in proximal RC.

Rare earth element patterns of selected samples (Table 6) of proximal and distal RC, normalized to the chondritic values (Mc Donough and Sun 1995) are displayed in Fig. 10a, b. These patterns show differing behavior between the proximal and distal RC. In proximal RC both light rare earth elements (LREE) and heavy rare earth elements (HREE) are depleted when compared with the fresh rocks (Fig. 10a), whereas in distal RC, REE patterns show enrichment in LREE and impoverishment in HREE (Fig. 10b).

Discussion

At La Fossa volcano and in the surrounding environment RC develop owing to the exposure of the ground surface to the effects of the fumarolic plume (Fulignati et al. 2002). The chemical composition of proximal RC is dominated by an abundance of silica ($SiO2 > 75$ wt%); compared with the fresh rocks there is a strong depletion in almost all other elements, including REE, Al_2O_3, Zr and TiO_2 generally considered as immobile. REE behavior in proximal RC supports this evidence, showing a general impoverishment both in LREE and HREE when compared with fresh rocks (Fig. 10a). All these characteristics are similar to those envisaged in the rocks affected by silicic alteration, found in the surficial, active, high-sulfidation hydrothermal system of La Fossa (Fulignati and Sbrana 1998; Fulignati et al. 1998, 1999). In consequence of the above we argue that the development of proximal RC is controlled by the same leaching processes that created the silicic facies. The condition required for these strong leaching processes to occur is a very low pH (< 2, Stoffregen 1987) for the fluids that interact with the outcropping rocks. We think that these fluids are produced by the direct interaction of volcaniclastic material with the acid fumarolic aerosol and by reaction with dew and rain water acidified by the absorption of the acid gases (SO_2, HCl, HF) of the fumarolic plume (Fulignati et al. 2002). The influence of the fumarolic plume in the genesis of proximal RC is furthermore reflected by the enrichment in several metals and trace elements (As, Pb, Bi, Ag, Te, Se, Cd and Sb), typically carried by the volcanic aerosol and found in proximal RC (Figs. 5, 6, 8, 9; Tables 1, 2, 5).

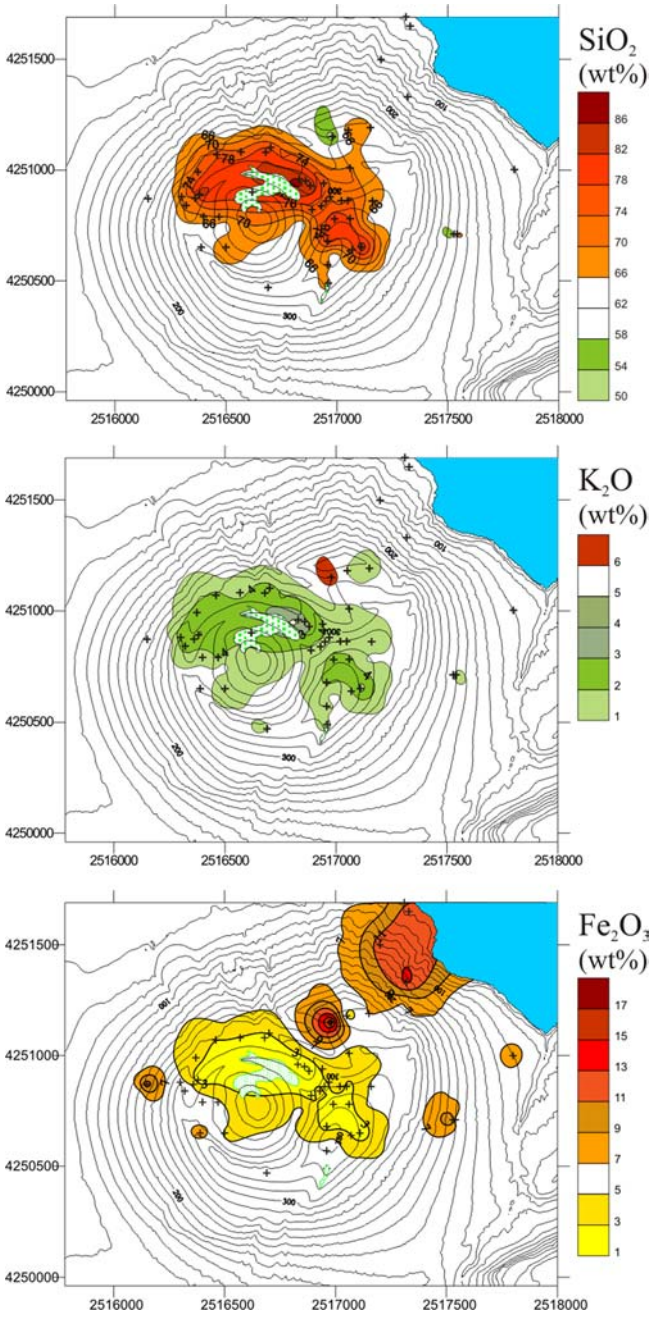

Fig. 4 Anomaly maps of SiO_2, K_2O and Fe_2O_3 for the RC of the La Fossa crater and surroundings

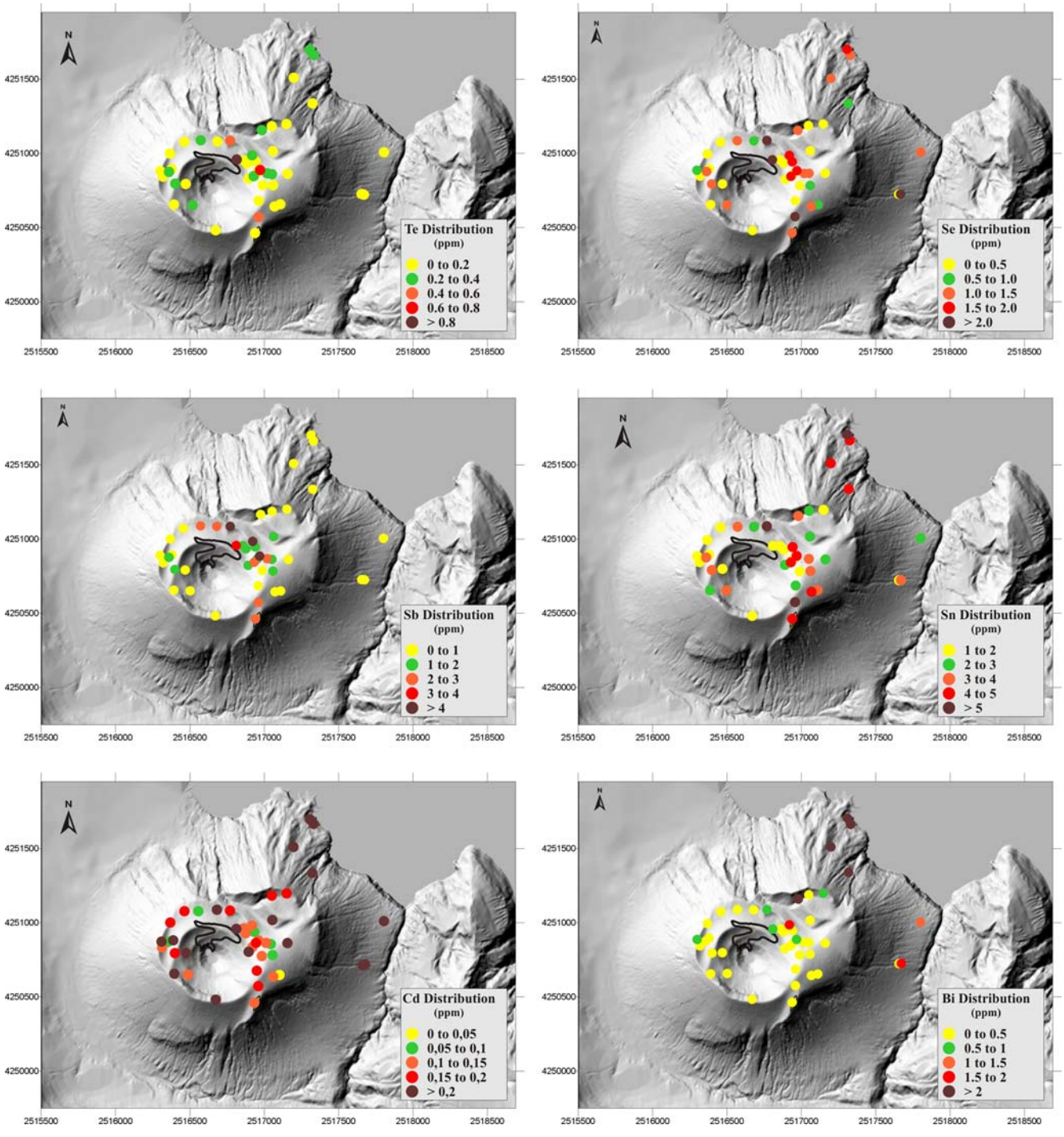

Fig. 5 Classed post maps showing the distribution of Te, Se, Sb, Sn, Ag and Tl in the RC of La Fossa volcano

Distal RC have a high Al_2O_3, Fe_2O_3, P_2O_5 and SO_3 content and the strong silicification process seen in proximal RC is not developed. This suggests that the fluids involved in distal RC development are not extremely acid (pH > 2) as those involved in proximal RC formation. We observed anomalously high concentrations in metals and trace elements typically carried by the fumarolic plume (As, Pb, Sn, Cu, Te, Se, Bi, Tl, Sb) also in distal RC and, differing from the proximal RC, in La, Ce and V (Figs. 8, 9; Table 5). High Al, Fe, P and S contents can be explained as their fixation in alteration minerals of the alunite–jarosite group (Scott 1987) that are very abundant in the distal RC (Fulignati et al. 2002). The same explanation is proposed for the

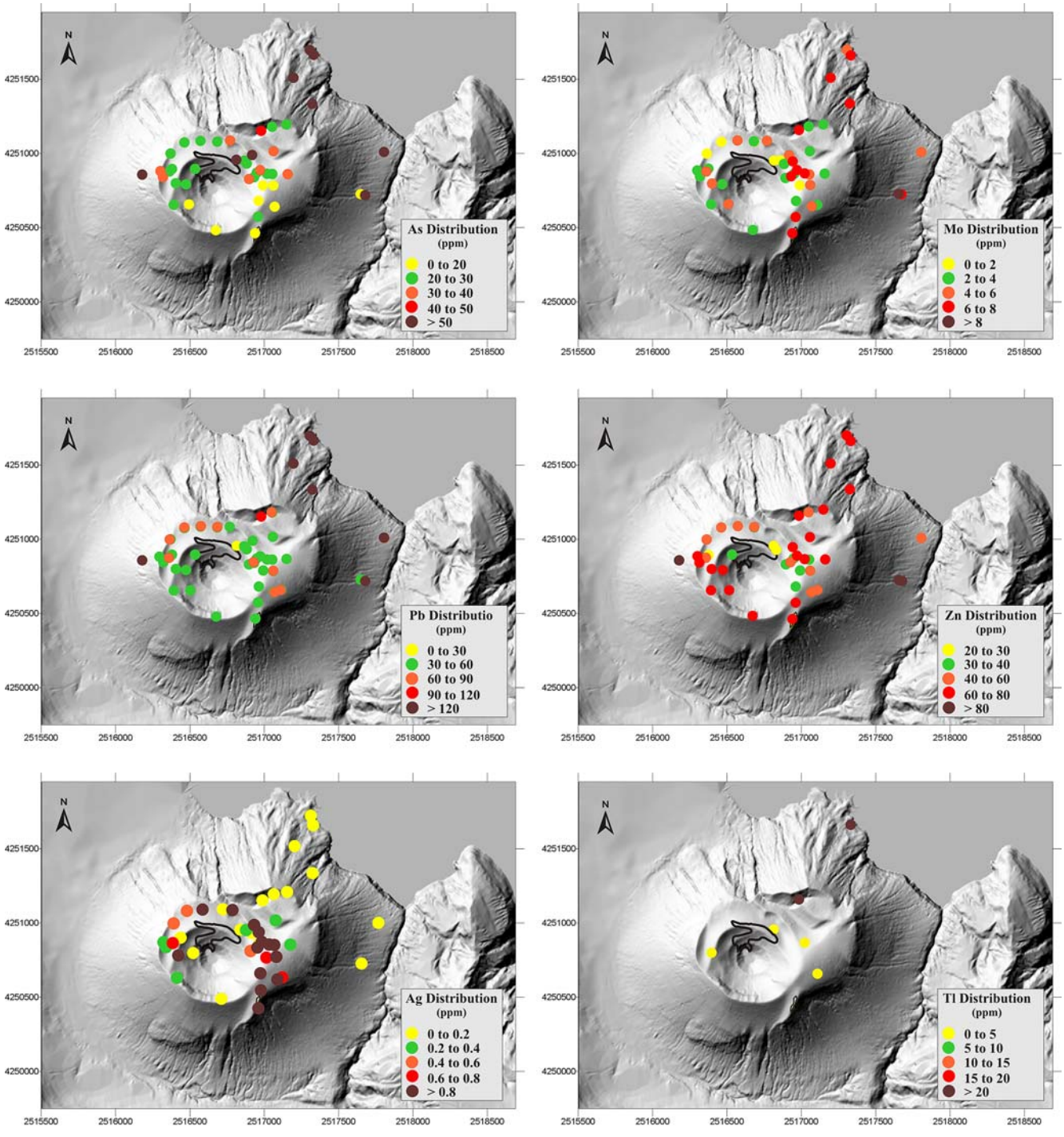

Fig. 6 Classed post maps showing the distribution of As, Mo, Pb, Zn, Cd and Bi in the RC of La Fossa volcano

presence of some trace elements such as Sr, Ba and LREE that can also be fixed in alunite–jarosite group minerals. These elements occur as a substitution for K in the large radius A site when considering the general formula $AB_3(XO_4)_2(OH)_6$. We also often found woodhousite–svanbergite solid solution [(Sr, Ca)$Al_3(SO_4)(PO_4)(OH)_6$] and florencite [(La, Ce)$Al_3(PO_4)_2(OH)_6$] associated with jarosite in the alteration paragenesis of distal RC (Table 3). The importance of alunite–jarosite minerals in the retention of LREE is confirmed by REE behavior in the distal RC. In fact, REE patterns in distal RC show a significant fractionation of the HREE with respect to LREE that are similar or enriched in concentration with respect to the fresh rock equivalent (Fig. 10b). These

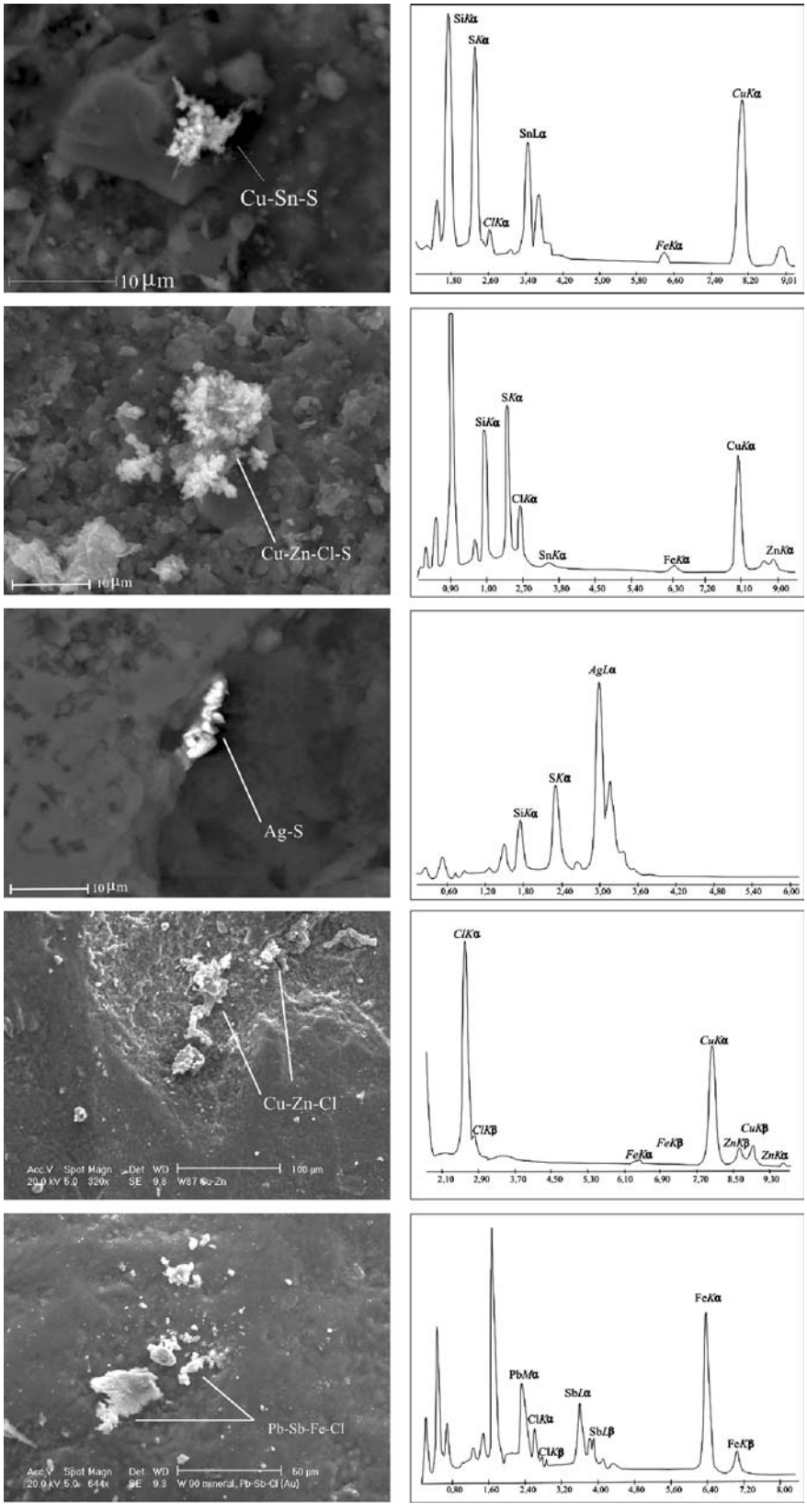

Fig. 7 SEM microphotographs and EDS spectra of metal-sulfide and/or chloride compounds found in the proximal and distal RC: **a** Cu–Zn–S compound in proximal RC; **b** Cu–Zn–S–Cl compound in proximal RC; **c** Ag–S compound in proximal RC; **d** Cu–Zn–Cl compound in distal RC; **e** Pb–Fe–Sb–Cl compound in distal RC

Table 3 Phases identified in proximal and distal RC through XRD and SEM-EDS investigation

RC	XRD	SEM-EDS
Proximal RC	Amorphous silica	Amorphous silica Barite Fe oxide-hydroxide containing: Cr, Zn, Ni, W and Cu Sulfur-bearing phases with: Cu–Zn, Ag, Cu–Sn and Cu–Bi Chloride-bearing phases with: Ca Chloride–Sulfur-bearing phases with: Cu–Zn Native elements: Au, Ag and W
Distal RC	Amorphous silica Jarosite	Amorphous silica Barite Jarosite: $KFe_3(SO_4)_2(OH)_6$ Fe oxide–hydroxide-containing: Cr, V, Zn, Sn, Ni and Cu Chloride-bearing phases with: Ca–K, Ca–Fe, Fe–Ni, Na–Zn, Pb–Sb–(Fe), Cu–Zn and Ni rare earth elements (REE)-bearing aluminium phosphate (fluorencite): REE $(Al_3(PO_4)_2(OH)_6$ Fe-REE phosphate–sulfate Fe phosphate Native elements: Au, Ag, Hg and traces of Se and As

Table 4 Composition of reference rock for proximal and distal RC

	Proximal RC	Distal RC
Bi	0.15	0.15
Ag	0.108	0.108
Se	0.086	0.086
Te	0.022	0.021
Sn	3.0	3.0
Sb	1.0	1.0
Pb	31	25
As	15	12
Tl	0.8	0.25
Cd	0.069	0.069
La	75	75
Ce	145	92.5
V	45	95
Mo	7.5	6.0
Ni	4.6	14.6
Cu	56	70
Zn	65	65

Table 5 Ranges of enrichment factors for Bi, Cd, Ag, Se, Te, Sn, Sb, Pb, As, Tl, Cd, La, Ce, V, Mo, Ni, Cu and Zn in proximal and distal RC (first number is the average value, second number is the highest value)

	Proximal RC	Distal RC
Bi	6.0×10^{-1}–1.1×10^{1}	8.2×10^{0}–1.8×10^{2}
Ag	5.3×10^{0}–4.1×10^{1}	9.9×10^{0}–2.7×10^{1}
Se	< ld–1.2×10^{3}	< ld–7.5×10^{1}
Te	< ld–7.0×10^{2}	< ld–4.9×10^{1}
Sn	6.0×10^{-2}–2.0×10^{0}	5.0×10^{-1}–1.8×10^{0}
Sb	3.0×10^{-1}–1.1×10^{1}	5.6×10^{-1}–1.9×10^{0}
Pb	1.0×10^{-1}–6.0×10^{0}	3.7×10^{0}–4.5×10^{1}
As	6.0×10^{-1}–1.8×10^{1}	2.0×10^{0}–2.0×10^{1}
Tl	5.0×10^{-1}–1.3×10^{1}	1.3×10^{1}–3.4×10^{2}
Cd	5.0×10^{-1}–1.3×10^{1}	1.8×10^{0}–9.1×10^{0}
La	3.7×10^{-1}–2.0×10^{0}	2.8×10^{0}–7.0×10^{0}
Ce	3.0×10^{-1}–1.6×10^{0}	3.0×10^{0}–7.7×10^{0}
V	4.7×10^{-1}–1.0×10^{0}	1.2×10^{0}–2.6×10^{0}
Mo	1.5×10^{-1}–1.4×10^{0}	9.0×10^{-1}–5.0×10^{0}
Ni	8.0×10^{-1}–3.8×10^{0}	7.0×10^{-1}–1.0×10^{1}
Cu	2.4×10^{-1}–1.4×10^{0}	2.0×10^{0}–5.0×10^{0}
Zn	1.2×10^{-1}–1.4×10^{0}	1.0×10^{0}–2.0×10^{0}

patterns are typical of the advanced argillic alteration facies which is characterized by an abundance of alunite–jarosite group minerals (Arribas et al. 1995; Fulignati et al. 1999). We conversely argue that the high concentration in trace elements, which are likely to form more volatile compounds (As, Tl, Pb, Bi, Cu, Cd, Te and Se) found in distal RC, is mainly to be attributed to the transport of these elements in the atmosphere and their subsequent deposition to the ground from the volcanic aerosols originated by the passive degassing of La Fossa volcano. This is supported by the occurrence of chloride-bearing compounds enriched in Se, Sn, Sb, Pb, As, Cu, Ag, Hg, Zn and Ni (Table 3; Fig. 7) on the surface of proximal RC. The possibility that these positive anomalies might be due to the leaching of the outcropping rocks and subsequent re-deposition of trace elements in distal RC is unlikely because of the very low concentrations of most of these elements in the unaltered rocks. Such a process would consequently need the involvement of unreasonably high rock volumes. The deposition from leaching solutions may account for, or may significantly contribute to, the moderately positive anomalies of V, Cr, Co and Ni. These elements are in fact relatively abundant in the Vulcano-unaltered rocks and may coprecipitate with goethite (Thurnber and Wildman 1979) or may form compounds with humic acids (Mantoura et al. 1978). These elements can, furthermore, be adsorbed onto iron hydroxides and clay minerals (Chapman et al. 1983). The close association between V, Cr, Co and Fe hydroxides is suggested by the occurrence of several goethites having significant amounts of Cr, V, Zn, Sn, Ni and Cu in distal RC (Table 3). However, we cannot exclude a possible direct contribution from the volcanic plume for Ni, and Fe

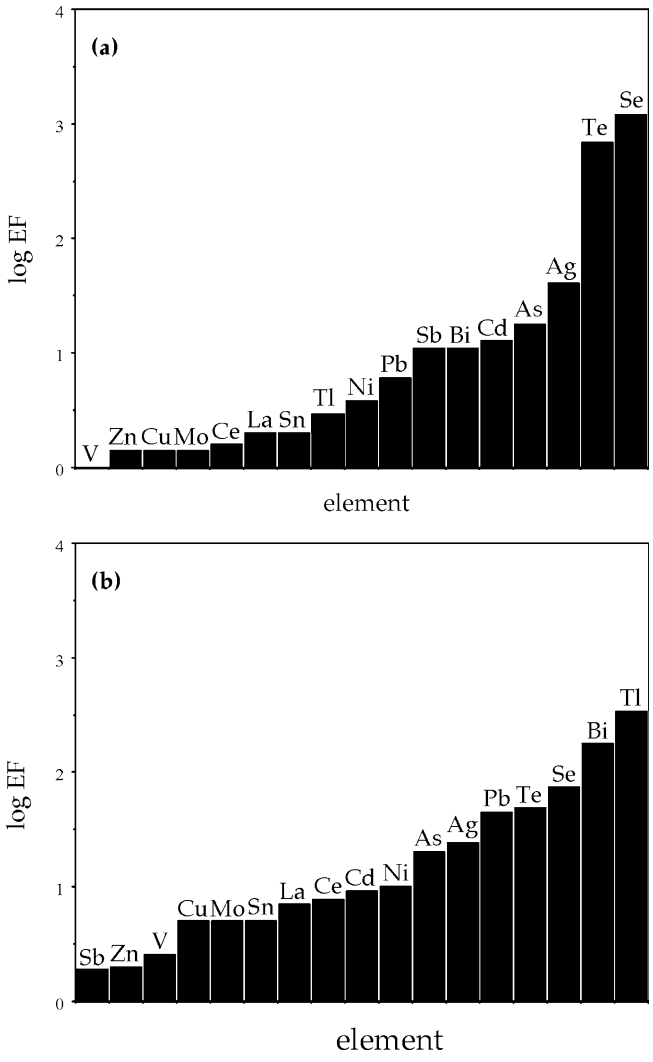

Fig. 8 Maximum enrichment factors (EF) of trace elements in the proximal (**a**) and distal (**b**) RC

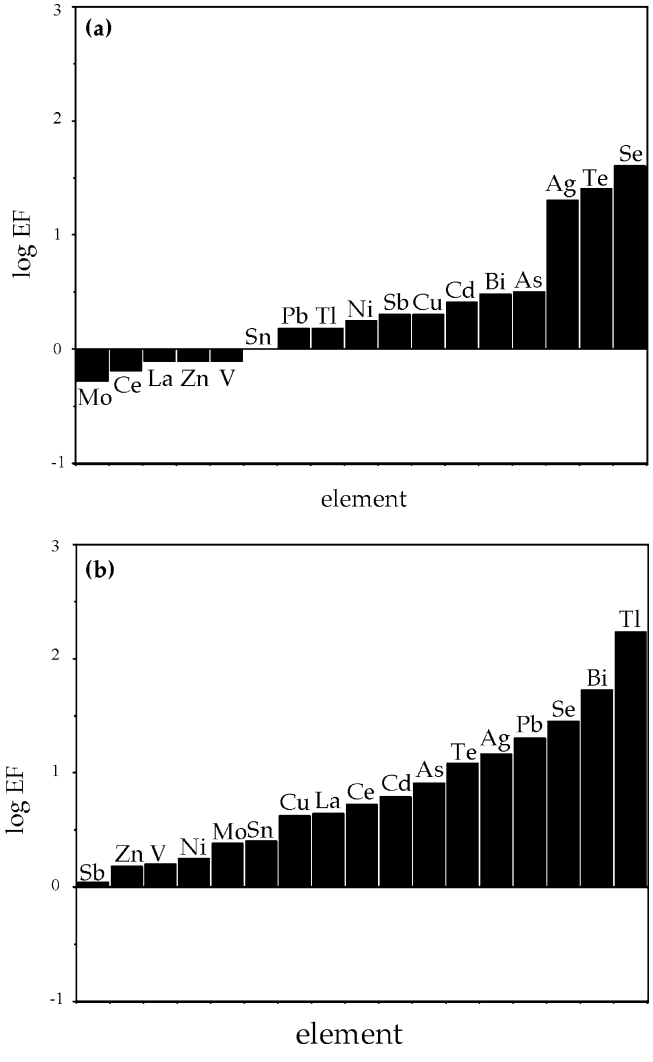

Fig. 9 Mean EF of trace elements in the proximal (**a**) and distal (**b**) RC

also. The occurrence of Ni- and Fe-bearing chloride phases in distal RC may support this hypothesis.

Even though the calculated EF values for trace elements, typically enriched in volcanic plumes, in proximal and distal RC are rather low when compared to those reported for fumarole condensates, sublimates and incrustations elsewhere (up to 10^5–10^6; Zoller et al. 1983; Symonds et al. 1987; Taran et al. 1995), they are significant and comparable to those found in modern tephra-fall deposit leachates (Armienta et al. 2002). EF values in RC suggested a fractionation amongst the trace elements (Figs. 8, 9; Table 5), with some elements that are more enriched in proximal RC (Te, Se, Ag, Sb) and other (Pb, Bi, Cd, As, Tl) enriched in distal RC. This selective behavior might reflect differences in the deposition temperature that prevents the transport of some elements far from the magmatic source (Symonds et al. 1987; Bernard et al. 1990). Another possibility, which does not necessarily exclude the first, is that the differing enrichments are functions of the different conditions of proximal and distal RC formation (mainly a different pH), which would preferentially either allow or prevent the combination of trace elements in RC.

Conclusions

This paper presents the results of a study on the effects caused by the fumarolic plume of a passively degassing volcano on the surrounding environment. In particular we consider the role played by the fumarolic plume in the genesis of RC and in the introduction and redistribution of trace elements in the surficial environment.

Significant positive anomalies for a wide variety of metals and trace elements were observed in both

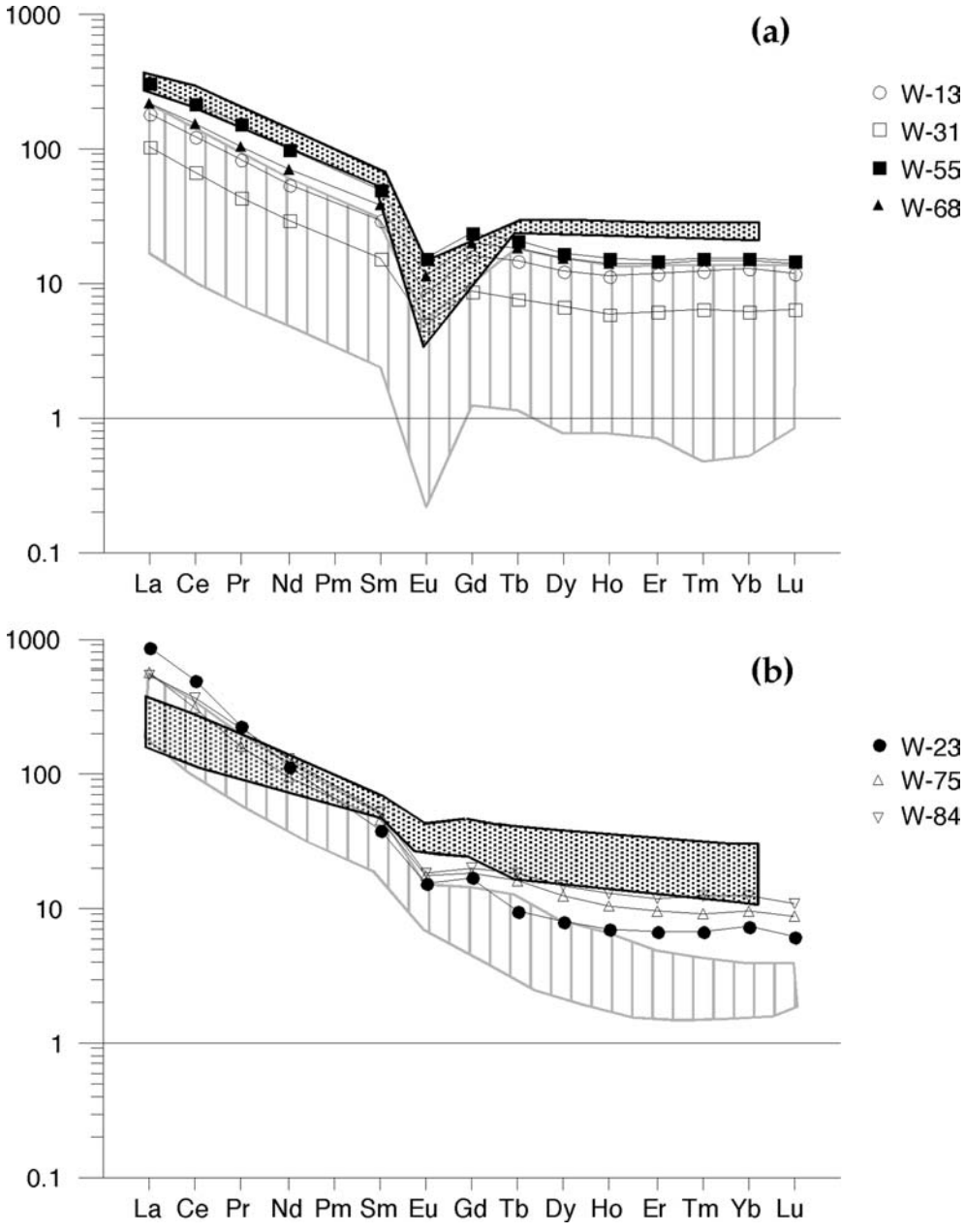

Fig. 10 Chondrite-normalized REE patterns of samples from the proximal RC (**a**) and distal RC (**b**), compared to unaltered equivalent rocks (*gray areas*; values were taken from Del Moro et al. 1998) and hydrothermally altered rocks (*ruled areas*; values were taken from Fulignati et al. 1999) from the silicic alteration (**a**) and advanced argillic alteration (**b**) facies of Vulcano, respectively. Chondrite-normalizing values from Mc Donough and Sun (1995)

distal and proximal RC. Most of these anomalies are interpreted as being the result of the transport and subsequent deposition in the plume of trace elements that are likely to form more volatile compounds. This indicates that RC are an important factor in the fixation and redistribution of metals and trace elements in the environment surrounding La Fossa crater.

Significant compositional differences were observed between the proximal and distal RC developed on Vulcano Island. Two main processes seem to control the geochemistry of RC. One is represented by the leaching and subsequent deposition of elements from the proximal toward the distal RC; the other is the direct input of trace elements carried by the volcanic aerosol emitted by La Fossa fumarolic field. The proximal RC composition is the result of strong leaching processes under extremely acid ($pH < 2$) conditions on outcropping pyroclastic deposits, coupled with the direct input of several metals and trace elements contributed by the fumarole plume. The distal RC composition mainly results from the direct input of elements from the fumarolic plume (as in proximal RC) and the precipitation of elements from the surficial solutions that have been involved in the leaching processes that generate

Table 6 Representative REE analysis of proximal and distal RC

	Proximal RC				Distal RC		
	W13	W31	W55	W68	W23	W75	W84
La	43	25.3	75	53	206	132	128
Ce	75	41	136	93	304	193	226
Pr	7.7	4.2	14.1	9.7	21.4	15.1	20.2
Nd	25.0	13.7	46	32	53	44	60
Sm	4.3	2.33	7.5	5.7	5.7	6.6	7.8
Eu	0.47	0.28	0.86	0.65	0.85	0.97	1.05
Gd	3.2	1.71	4.8	4.0	1.47	3.6	3.9
Tb	0.54	0.28	0.76	0.67	0.35	0.57	0.67
Dy	3.1	1.65	4.2	3.8	1.96	3.1	3.6
Ho	0.64	0.33	0.86	0.78	0.39	0.57	0.70
Er	1.88	0.99	2.37	2.23	1.06	1.55	1.92
Tm	0.31	0.16	0.39	0.37	0.17	0.23	0.30
Yb	2.10	1.00	2.54	2.38	1.16	1.53	1.99
Lu	0.30	0.16	0.37	0.35	0.15	0.22	0.28

proximal RC. The occurrence of this process is supported by the fact that some of the strongest positive anomalies in the distal RC are located inside rills that channel the surficial waters on the eastern flank of the La Fossa volcano.

The widespread development of RC on the volcanic products of the last eruption of La Fossa volcano (1888–1890) suggests that the process of RC formation is rapid taking place over a time period in the order of some decades. The high concentration of metals in RC is thus not necessarily the result of metal accumulation over thousands of years but it can be developed in a relatively few years, comparable to a median human age. This suggests a high output rate of trace elements from the fumarolic field. We finally remark that most of the trace elements (especially Pb, As, Tl, Bi, Te, Se and Cd) enriched in the RC of Vulcano, are highly toxic and potentially dangerous to health at high concentrations (Allen et al. 2000). Their positive anomalous presence in the RC indicate that the atmospheric metal injection from the quiescently degassing La Fossa volcano and the subsequent deposition and remobilization by means of surficial waters may represent an environmental hazard that should be taken into account in the evaluation of the potential impact of volcanic air pollution on human health in Vulcano Island. For this reason further work will be required to better understand the concentration and mobility of toxic metals and trace elements in the air and in Vulcano groundwater.

Acknowledgments Many thanks are due to F. Carrot and A. Michel for help in the ICP-MS analyses at Laboratoire Pierre Sue (Gif Sur Yvette, France). We are also grateful to M. Menichini for XRF analyses and M. D'Orazio for help in ICP-MS analyses in the Dipartimento di Scienze della Terra (Pisa, Italy). The authors are grateful to Prof. Jorg Matschullat for reviewing the manuscript. This research was supported financially by a Gruppo Nazionale per la Vulcanologia-Instituto Nazionale di Geofisica e Vulcanologia grant.

References

Allard P, Aiuppa A, Loyer H, Carrot F, Gaudry A, Pinte G, Michel A, Dongarrà G (2000) Acid gas and metal emission rates during long-lived basalt degassing at Stromboli volcano. Geophys Res Lett 27:1207–1210

Allen AG, Baxter PJ, Ottley CJ (2000) Gas and particle emission from Soufrière Hills Volcano, Montserrat, West Indies: characterization and health assessment. Bull Volcanol 62:8–19

Armienta MA, Martin-Del-Pozzo AL, Espinasa R, Cruz O, Ceniceros N, Aguayo A, Butron MA (1998) Geochemistry of ash leachates during the 1994–1996 activity of Popocatèpetl volcano. Appl Geochem 13:841–850

Armienta MA, De la Cruz-Reyna S, Morton O, Cruz O, Ceniceros N (2002) Chemical variations of tephra-fall deposit leachates for three eruptions from Popocatèpetl volcano. J Volcanol Geotherm Res 113:61–80

Arribas A Jr, Cunningham CG, Rytuba JJ, Rye RO, Kelly WC, Podwisocki MH, McKee EH, Tosdal RM (1995) Geology, geochronology, fluid inclusions, and isotope geochemistry of the Rodalquilar gold alunite deposit, Spain. Econ Geol 90:795–822

Barberi F, Neri G, Valenza M, Villari L (1991) 1987–1990 unrest at Vulcano. Acta Vulcanol 1:95–106

Bernard A, Symonds RB, Rose WI (1990) Volatile transport and deposition of Mo, W and Re in high temperature magmatic fluids. Appl Geochem 5:317–326

Bolognesi L, D'Amore F (1993) Isotopic variation of the hydrothermal system on Vulcano Island, Italy. Geochim Cosmochim Acta 57:2069–2082

Buat-Menard P, Arnold M (1978) The heavy metal chemistry of atmospheric particulate matter emitted by Mount Etna volcano. Geophys Res Lett 5:245–248

Capasso G, Favara R, Inguaggiato S (1997) Chemical features and isotopic composition of gaseous manifestations on Vulcano Island, Aeolian Islands, Italy: an interpretative model of fluid circulation. Geochim Cosmochim Acta 61:3425–3440

Chapman BM, Jones DR, Jung RF (1983) Processes controlling metal ion attenuation in acid mine drainage streams. Geochim Cosmochim Acta 47:1957–1973

Cheynet B, Dall'Aglio M, Garavelli A, Grasso MF, Vurro F (2000) Trace elements from fumaroles at Vulcano Island (Italy): rates of transport and a thermochemical model. J Volcanol Geotherm Res 95:273–283

Chiodini G, Cioni R, Marini L (1993) Reactions governing the chemistry of crater fumaroles from Vulcano Island, Italy, and implications for volcanic surveillance. Appl Geochem 8:357–371

Chiodini G, Cioni R, Marini L, Panichi C (1995) Origin of the fumarolic fluids of Vulcano Island, Italy and implications for volcanic surveillance. Bull Volcanol 57:99–110

Clocchiatti R, Del Moro A, Gioncada A, Joron JL, Mosbah M, Pinarelli L, Sbrana A (1994) Assessment of a shallow magmatic system: the case of the 1888–90 eruption, Vulcano Island, Italy. Bull Volcanol 56:466–486

Del Moro A, Gioncada A, Pinarelli L, Sbrana A, Joron JL (1998) Sr, Nd, and Pb isotope evidence of open system evolution at Vulcano (Aeolian Arc, Italy). Lithos 43:81–106

Delmelle P (2003) Environmental impacts of tropospheric volcanic gas plumes. In: Oppenheimer C, Pyle DM, Barclay J (eds) Volcanic degassing. Geol Soc London Special Publ 213:381–399

Fulignati P, Sbrana A (1998) Presence of native gold and tellurium in the active high-sulfidation hydrothermal system of the La Fossa volcano (Vulcano, Italy). J Volcanol Geotherm Res 86:187–198

Fulignati P, Gioncada A, Sbrana A (1998) Geologic model of the magmatic-hydrothermal system of Vulcano (Aeolian Island, Italy). Mineral Petrol 62:195–222

Fulignati P, Gioncada A, Sbrana A (1999) Rare-earth element (REE) behaviour in the alteration facies of the active magmatic-hydrothermal system of Vulcano (Aeolian Islands, Italy). J Volcanol Geotherm Res 88:325–342

Fulignati P, Sbrana A, Luperini W, Greco V (2002) Formation of rock coatings induced by the acid fumarole plume of the passively degassing volcano of La Fossa (Vulcano Island, Italy). J Volcanol Geotherm Res 115:397–410

Garavelli A, Laviano R, Vurro F (1997) Sublimate deposition from hydrothermal fluids at the Fossa crater, Vulcano, Italy. Eur J Mineral 9:423–432

Gauthier PJ, Le Cloarec MF (1998) Variability of alkali and heavy metal fluxes released by Mt. Etna volcano, Sicily, between 1991 and 1995. J Volcanol Geotherm Res 81:311–326

Gemmel BJ (1987) Geochemistry of metallic trace elements in fumarolic condensates from Nicaraguan and Costa Rican volcanoes. J Volcanol Geotherm Res 33:161–181

Gioncada A, Clocchiatti R, Sbrana A, Bottazzi P, Massare D, Ottolini L (1998) A study of melt inclusions at Vulcano (Aeolian islands, Italy): insight on the primitive magmas and on the volcanic feeding system. Bull Volcanol 60:286–306

Govindaraju K (1994) 1994 compilation of working values and sample description for 383 geostandards. Geostand Newslett 18:1–158

Grasso MF, Clocchiatti R, Carrot F, Deschamps C, Vurro F (1999) Lichens as bioindicators in volcanic areas: Mt. Etna and Vulcano island (Italy). Environ Geol 37:207–217

Hedenquist JW (1995) The ascent of magmatic fluid: discharge versus mineralization. In: Thompson JFH (ed) Magmas fluids and ore deposits. Mineralogical Association of Canada Short Course 23:263–289

Hedenquist JW, Aoki M, Shinohara H (1994) Flux of volatiles and ore-forming metals from the magmatic-hydrothermal system of Satsuma Iwojima volcano. Geology 22:585–588

Hinkley TK, Le Cloarec MF, Lambert G (1994) Fractionation of families of major, minor, and trace metals across the melt-vapor interface in volcanic exhalations. Geochim Cosmochim Acta 58:3255–3263

Hinkley TK, Lamothe PJ, Wilson SA, Finnegan DL, Gerlach TM (1999) Metal emissions from Kilauea, and a suggested revision of the estimated worldwide metal output by quiescent degassing of volcanoes. Earth Planet Sci Lett 170:315–325

Kavalieris I (1994) High Au, Ag, Mo, Pb, V and W content of fumarolic deposits at Merapi volcano, central Java, Indonesia. J Geochem Expl 50:479–491

Keller J (1980) The island of Vulcano. Rend Soc It Mineral Petr 36:369–414

Korzhinsky MA, Tkachenko SI, Shmulovich KI, Taran YA, Steinberg GS (1994) Discovery of a pure rhenium mineral at Kudriavy volcano. Nature 369:51–52

Larocque ACL, Stimac JA, Siebe C (1998) Metal-residence sites in lavas and tuffs from volcan Popocatepetl, Mexico: implications for metal mobility in the environment. Environ Geol 33:197–208

Le Cloarec MF, Allard P, Ardouin B, Giggenbach WF, Sheppard DS (1992) Radioactive isotopes and trace elements in gaseous emissions from White Island, New Zealand. Earth Planet Sci Lett 108:19–28

Le Guern R (1988) Ecoulement gazeux reactifs a haute temperature, measures et modelisation. Ph. D. Thesis, University of Paris VII

Mantoura RFC, Dickson A, Riley JP (1978) The complexation of metals with humic materials in natural waters. Estuarine Coastal Mar Sci 6:387–408

Matsumoto A, Hinkley TK (2001) Trace metal suites in Antartic pre-industrial ice are consistent with emissions from quiescent degassing of volcanoes worldwide. Earth Planet Sci Lett 186:33–43

Mc Donough WF, Sun SS (1995) The composition of the earth. Chem Geol 120:223–253

Murozumi M (1992) Vertical profiles of heavy metals in the oceans, Symposium on topics on global geochemistry, Division of Geological and Planet Science, California Institute of Technology, Abstracts with program 6 (abstr.)

Nriagu JO (1989) A global assessment of natural sources of atmospheric trace metals. Nature 338:47–49

Pyle DM, Mather TA (2003) The importance of volcanic emissions for the global atmospheric mercury cycle. Atmos Environ 37:5115–5124

Quisefit JP, Toutain JP, Bergametti G, Javoy M, Cheynet B, Pearson A (1989) Evolution versus cooling of gaseous volcanic emissions from Momotombo volcano, Nicaragua: thermodynamical model and observations. Geochim Cosmochim Acta 53:2591–2608

Scott KM (1987) Solid solution in, and classification of, gossan-derived members of the alunite–jarosite family, northwest Queensland, Australia. Am Mineral 72:178–187

Sortino F, Bichler M (1997) Elementi in traccia: genesi e trasporto nei gas fumarolici a Vulcano (In Italian). In: LaVolpe L, Dellino P, Nuccio M, Privitera E, Sbrana A (eds) Progetto Vulcano, risultati delle attività di ricerca 1993–1995. Felici Editor, Pisa, pp 147–152

Stoffregen R (1987) Genesis of acid-sulfate alteration and Au–Cu–Ag mineralization at Summitville, Colorado. Econ Geol 82:1575–1591

Symonds RB (1992) Getting the gold from the gas: how recent advances in volcanic-gas research have provided new insight on metal transport in magmatic fluids. In: Hedenquist JW (ed) Magmatic contributions to hydrothermal systems. Report No. 279, Geological Survey of Japan, Tsukuba, pp 170–175

Symonds RB, Reed MH (1993) Calculation of multicomponent chemical equilibria in gas–solid–liquid systems: calculation methods, thermochemical data, and applications to studies of high-temperature volcanic gases with examples from mount St. Helens. Am J Sci 293:758–864

Symonds RB, Rose WI, Reed MH, Lichte FE, Finnegan DL (1987) Volatilization, transport and sublimation of metallic and non-metallic elements in high temperature gases at Merapi Volcano, Indonesia. Geochim Cosmochim Acta 51:2083–2101

Symonds RB, Rose WI, Gerlach TM, Briggs PH, Harmon RS (1990) The evaluation of gases, condensates and SO2 emissions from Augustine volcano, Alaska: the degassing of a Cl-rich volcanic system. Bull Volcanol 52:355–374

Symonds RB, Rose WI, Bluth GJS, Gerlach TM (1994) Volcanic-gas studies: methods results and applications. In: Carroll MR, Holloway JR (eds) Volatiles in magmas. Rev Mineral 26:1–66

Taran YA, Hedenquist JW, Korzhinsky MA, Tcachenko SI, Shmulovich KI (1995) Geochemistry of magmatic gases from Kudryavy volcano, Iturup, Kurile Islands. Geochim Cosmochim Acta 59:1749–1761

Taran YA, Bernard A, Gavilanes J-C, Africano F (2000) Native gold in mineral precipitates from high-temperature volcanic gases of Colima volcano, Mexico. Appl Geochem 15:337–346

Thurnber MR, Wildman JE (1979) Supergene alteration of sulphides. IV. Laboratory study of weathering of nickel ores. Chem Geol 24:97–110

Varrica D, Aiuppa A, Dongarrà G (2000) Volcanic and anthropogenic contribution to heavy metal content in lichens from Mt. Etna and Vulcano island (Sicily). Environ Pollut 108:153–162

Ventura G (1994) Tectonics, structural evolution and caldera formation on Vulcano island (Aeolian Archipelago, Southern Tyrrenian). J Volcanol Geotherm Res 60:206–224

Zelenski M, Bortnikova S (2005) Sublimate speciation at Mutnovsky volcano, Kamchatka. Eur J Mineral 17:107–118

Zoller WH, Parrington JR, Phelan Kotra JM (1983) Iridium enrichment in airborne particles from Kilauea volcano: January 1983. Science 222:1118–1121

Zreda-Gostynska G, Kyle PR, Finnegan D, Meeker Prestbo K (1997) Volcanic gas emissions front Mount Erebus and their impact on the Antarctic environment. J Geophys Res 102:15039–15055